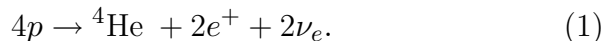


SOLAR NEUTRINOS

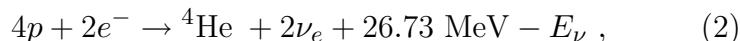
Revised November 2003 by K. Nakamura (KEK, High Energy Accelerator Research Organization, Japan).

1. Introduction

The Sun is a main-sequence star at a stage of stable hydrogen burning. It produces an intense flux of electron neutrinos as a consequence of nuclear fusion reactions whose combined effect is



Positrons annihilate with electrons. Therefore, when considering the solar thermal energy generation, a relevant expression is



where E_ν represents the energy taken away by neutrinos, with an average value being $\langle E_\nu \rangle \sim 0.6$ MeV. The neutrino-producing reactions which are at work inside the Sun are enumerated in the first column in Table 1. The second column in Table 1 shows abbreviation of these reactions. The energy spectrum of each reaction is shown in Fig. 1.

Observation of solar neutrinos directly addresses the theory of stellar structure and evolution, which is the basis of the standard solar model (SSM). The Sun as a well-defined neutrino source also provides extremely important opportunities to investigate nontrivial neutrino properties such as nonzero mass and mixing, because of the wide range of matter density and the great distance from the Sun to the Earth.

A pioneering solar neutrino experiment by Davis and collaborators using ${}^{37}\text{Cl}$ started in the late 1960's. From the very beginning of the solar-neutrino observation [1], it was recognized that the observed flux was significantly smaller than the SSM prediction, provided nothing happens to the electron neutrinos after they are created in the solar interior. This deficit has been called “the solar-neutrino problem.”

In spite of the challenges by the chlorine and gallium radiochemical experiments (GALLEX, SAGE, and GNO) and water-Cherenkov experiments (Kamiokande and Super-Kamiokande), the solar-neutrino problem had persisted for more than 30 years.

However, there have been remarkable developments in the past few years and now the solar-neutrino problem has been finally solved.

In 2001, the initial result from SNO (Sudbury Neutrino Observatory) [2], a water Cherenkov detector with heavy water, on the solar-neutrino flux measured via charged-current (CC) reaction, $\nu_e d \rightarrow e^- pp$, combined with the Super-Kamiokande's high-statistics flux measurement via νe elastic scattering [3], provided direct evidence for flavor conversion of solar neutrinos [2]. Later in 2002, SNO's measurement of the neutral-current (NC) rate, $\nu d \rightarrow \nu pn$, and the updated CC result further strengthened this conclusion [4].

The most probable explanation which can also solve the solar-neutrino problem is neutrino oscillation. At this stage, the LMA (large mixing angle) solution was the most promising. However, at 3σ confidence level, LOW (low probability or low mass) and/or VAC (vacuum) solutions were allowed depending on the method of analysis (see Sec. 3.6). LMA and LOW are solutions of neutrino oscillation in matter [5,6] and VAC is a solution of neutrino oscillation in vacuum. Subsequently, experiments have excluded vacuum oscillations and there exists strong evidence that matter effects are required in the solution to the solar-neutrino problem.

In December 2002, KamLAND (Kamioka Liquid Scintillator Anti-Neutrino Detector), a terrestrial $\bar{\nu}_e$ disappearance experiment using reactor neutrinos, observed clear evidence of neutrino oscillation with the allowed parameter region overlapping with the parameter region of the LMA solution [7]. Assuming CPT invariance, this result directly implies that the true solution of the solar ν_e oscillation has been determined to be LMA. A combined analysis of all the solar-neutrino data and KamLAND data significantly constrained the allowed parameter region. Inside the LMA region, the allowed region splits into two bands with higher Δm^2 and lower Δm^2 .

More recently, in September, 2003, SNO reported [8] results on solar-neutrino fluxes observed with NaCl added in heavy water: this improved the sensitivity for the detection of the NC reaction. A global analysis of all the solar neutrino data

combined with the KamLAND data further reduced the allowed region to the lower Δm^2 band with the best fit point of $\Delta m^2 = 7.1 \times 10^{-5} \text{ eV}^2$ and $\theta = 32.5$ degrees [8].

2. Solar Model Predictions

A standard solar model is based on the standard theory of stellar evolution. A variety of input information is needed in the evolutionary calculations. The most elaborate SSM, BP2000 [9], is presented by Bahcall *et al.* who define their SSM as the solar model which is constructed with the best available physics and input data. Though they used no helioseismological constraints in defining the SSM, the calculated sound speed as a function of the solar radius shows an excellent agreement with the helioseismologically determined sound speed to a precision of 0.1% rms throughout essentially the entire Sun. This greatly strengthens the confidence in the solar model. The BP2000 predictions [9] for the flux and contributions to the event rates in chlorine and gallium solar-neutrino experiments from each neutrino-producing reaction are listed in Table 1. The solar-neutrino spectra shown in Fig. 1 also resulted from the BP2000 calculations [9].

Other recent solar-model predictions for solar-neutrino fluxes were given by Turck-Chieze *et al.* [10] Their model is based on the standard theory of stellar evolution where the best physics available is adopted, but some fundamental inputs such as the pp reaction rate and the heavy-element abundance in the Sun are seismically adjusted within the commonly estimated errors aiming at reducing the residual differences between the helioseismologically-determined and the model-calculated sound speeds. Their predictions for the event rates in chlorine and gallium solar-neutrino experiments as well as ^8B solar-neutrino flux are shown in the last line in Table 2, where the BP2000 predictions [9] are also shown in the same format. As is apparent from this table, the predictions of the two models are remarkably consistent.

The SSM predicted ^8B solar-neutrino flux is proportional to the low-energy cross section factor $S_{17}(0)$ for the $^7\text{Be}(p,\gamma)^8\text{B}$ reaction. The BP2000 [9] and Turck-Chieze *et al.* [10] models adopted $S_{17}(0) = 19_{-2}^{+4} \text{ eV}\cdot\text{b}$. Inspired by the recent precise

measurement of the low-energy cross section for the ${}^7\text{Be}(p,\gamma){}^8\text{B}$ reaction by Junghans *et al.* [11], Bahcall *et al.* [12] calculated the (BP2000 + New ${}^8\text{B}$) SSM predictions using $S_{17}(0) = (22.3 \pm 0.9)$ eV·b. The results are: a ${}^8\text{B}$ solar-neutrino flux of $5.93(1.00^{+0.14}_{-0.15}) \times 10^6$ cm $^{-2}$ s $^{-1}$, a chlorine capture rate of $8.59^{+1.1}_{-1.2}$ SNU, and a gallium capture rate of 130^{+9}_{-7} SNU.

Table 1: Neutrino-producing reactions in the Sun (first column) and their abbreviations (second column). The neutrino fluxes and event rates in chlorine and gallium solar-neutrino experiments predicted by Bahcall, Pinsonneault and Basu [9] are listed in the third, fourth, and fifth columns respectively.

Reaction	Abbr.	BP2000 [9]		
		Flux (cm $^{-2}$ s $^{-1}$)	Cl (SNU*)	Ga (SNU*)
$pp \rightarrow de^+ \nu$	pp	$5.95(1.00^{+0.01}_{-0.01}) \times 10^{10}$	—	69.7
$pe^- p \rightarrow d\nu$	pep	$1.40(1.00^{+0.015}_{-0.015}) \times 10^8$	0.22	2.8
${}^3\text{He} p \rightarrow {}^4\text{He} e^+ \nu$	hep	9.3×10^3	0.04	0.1
${}^7\text{Be} e^- \rightarrow {}^7\text{Li} \nu + (\gamma)$	${}^7\text{Be}$	$4.77(1.00^{+0.10}_{-0.10}) \times 10^9$	1.15	34.2
${}^8\text{B} \rightarrow {}^8\text{Be}^* e^+ \nu$	${}^8\text{B}$	$5.05(1.00^{+0.20}_{-0.16}) \times 10^6$	5.76	12.1
${}^{13}\text{N} \rightarrow {}^{13}\text{C} e^+ \nu$	${}^{13}\text{N}$	$5.48(1.00^{+0.21}_{-0.17}) \times 10^8$	0.09	3.4
${}^{15}\text{O} \rightarrow {}^{15}\text{N} e^+ \nu$	${}^{15}\text{O}$	$4.80(1.00^{+0.25}_{-0.19}) \times 10^8$	0.33	5.5
${}^{17}\text{F} \rightarrow {}^{17}\text{O} e^+ \nu$	${}^{17}\text{F}$	$5.63(1.00^{+0.25}_{-0.25}) \times 10^6$	0.0	0.1
Total			$7.6^{+1.3}_{-1.1}$	128^{+9}_{-7}

* 1 SNU (Solar Neutrino Unit) = 10^{-36} captures per atom per second.

3. Solar Neutrino Experiments

So far, seven solar-neutrino experiments have published results. The most recent published results on the average event rates or flux from these experiments are listed in Table 2 and compared to the two recent solar-model predictions.

3.1. Radiochemical Experiments

Radiochemical experiments exploit electron neutrino absorption on nuclei followed by their decay through orbital electron capture. Produced Auger electrons are counted.

The Homestake chlorine experiment in USA uses the reaction



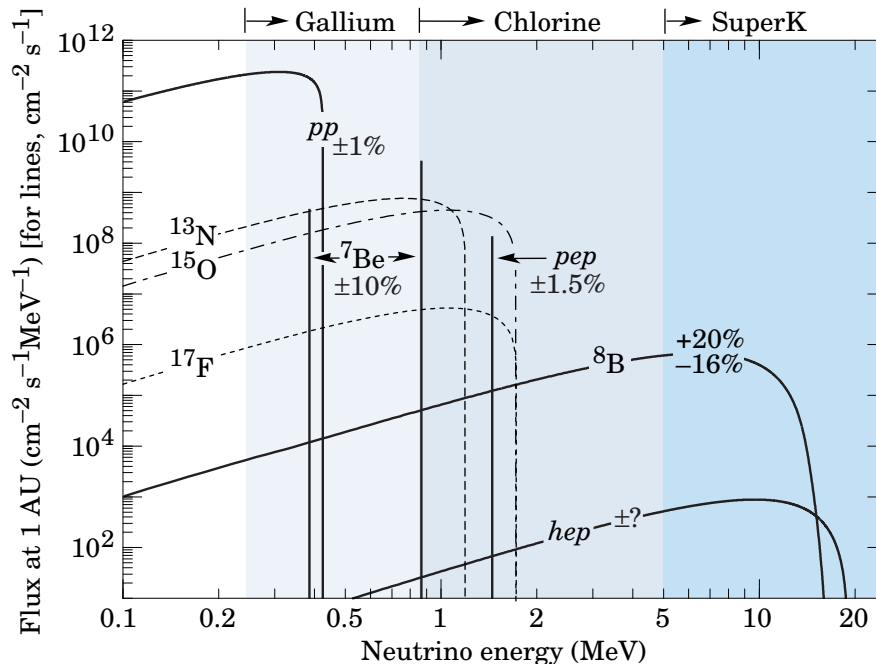


Figure 1: The solar neutrino spectrum predicted by the standard solar model. The neutrino fluxes from continuum sources are given in units of number $\text{cm}^{-2}\text{s}^{-1}\text{MeV}^{-1}$ at one astronomical unit, and the line fluxes are given in number $\text{cm}^{-2}\text{s}^{-1}$. Spectra for the pp chain, shown by the solid curves, are courtesy of J.N. Bahcall (2001). Spectra for the CNO chain are shown by the dotted curves, and are also courtesy of J.N. Bahcall (1995). See full-color version on color pages at end of book.

Three gallium experiments (GALLEX and GNO at Gran Sasso in Italy and SAGE at Baksan in Russia) use the reaction



The produced ${}^{37}\text{Ar}$ and ${}^{71}\text{Ge}$ atoms are both radioactive, with half lives ($\tau_{1/2}$) of 34.8 days and 11.43 days, respectively. After an exposure of the detector for two to three times $\tau_{1/2}$, the reaction products are chemically extracted and introduced into a low-background proportional counter, where they are counted

Table 2: Recent results from the seven solar-neutrino experiments and a comparison with standard solar-model predictions. Solar model calculations are also presented. The first and the second errors in the experimental results are the statistical and systematic errors, respectively.

	$^{37}\text{Cl} \rightarrow ^{37}\text{Ar}$ (SNU)	$^{71}\text{Ga} \rightarrow ^{71}\text{Ge}$ (SNU)	^8B ν flux ($10^6 \text{cm}^{-2} \text{s}^{-1}$)
Homestake			
(CLEVELAND 98)[13]	$2.56 \pm 0.16 \pm 0.16$	—	—
GALLEX			
(HAMPEL 99)[14]	—	$77.5 \pm 6.2^{+4.3}_{-4.7}$	—
GNO			
(ALTMANN 00)[15]	—	$65.8^{+10.2+3.4}_{-9.6-3.6}$	—
SAGE			
(ABDURASHI...02)[16]	—	$70.8^{+5.3+3.7}_{-5.2-3.2}$	—
Kamiokande			
(FUKUDA 96)[17]	—	—	$2.80 \pm 0.19 \pm 0.33^\dagger$
Super-Kamiokande			
(FUKUDA 02)[18]	—	—	$2.35 \pm 0.03^{+0.07}_{-0.06}^\dagger$
SNO (pure D ₂ O)			
(AHMAD 02)[4]	—	—	$1.76^{+0.06}_{-0.05} \pm 0.09^\ddagger$
	—	—	$2.39^{+0.24}_{-0.23} \pm 0.12^\dagger$
	—	—	$5.09^{+0.44+0.46*}_{-0.43-0.43}$
SNO (NaCl in D ₂ O)			
(AHMED 03)[8]	—	—	$1.59^{+0.08+0.06\ddagger}_{-0.07-0.08}$
	—	—	$2.21^{+0.31}_{-0.26} \pm 0.10^\dagger$
	—	—	$5.21 \pm 0.27 \pm 0.38^*$
(BAHCALL 01)[9]	$7.6^{+1.3}_{-1.1}$	128^{+9}_{-7}	$5.05(1.00^{+0.20}_{-0.16})$
(TURCK-CHIEZE 01)[10]	7.44 ± 0.96	127.8 ± 8.6	4.95 ± 0.72

* Flux measured via the neutral-current reaction.

† Flux measured via νe elastic scattering.

‡ Flux measured via the charged-current reaction.

for a sufficiently long period to determine the exponentially decaying signal and a constant background.

Solar-model calculations predict that the dominant contribution in the chlorine experiment comes from ^8B neutrinos, but ^7Be , pep , ^{13}N , and ^{15}O neutrinos also contribute. At present, the most abundant pp neutrinos can be detected only in gallium

experiments. Even so, according to the solar-model calculations, almost half of the capture rate in the gallium experiments is due to other solar neutrinos.

The Homestake chlorine experiment was the first to attempt the observation of solar neutrinos. Initial results obtained in 1968 showed no events above background with upper limit for the solar-neutrino flux of 3 SNU [1]. After introduction of an improved electronics system which discriminates signal from background by measuring the rise time of the pulses from proportional counters, a finite solar-neutrino flux has been observed since 1970. The solar-neutrino capture rate shown in Table 2 is a combined result of 108 runs between 1970 and 1994 [13]. It is only about 1/3 of the BP2000 prediction [9].

GALLEX presented the first evidence of pp solar-neutrino observation in 1992 [19]. Here also, the observed capture rate is significantly less than the SSM prediction. SAGE initially reported very low capture rate, $20_{-20}^{+15} \pm 32$ SNU, with a 90% confidence-level upper limit of 79 SNU [20]. Later, SAGE observed similar capture rate to that of GALLEX [21]. Both GALLEX and SAGE groups tested the overall detector response with intense man-made ^{51}Cr neutrino sources, and observed good agreement between the measured ^{71}Ge production rate and that predicted from the source activity, demonstrating the reliability of these experiments. The GALLEX Collaboration formally finished observations in early 1997. Since April, 1998, a newly defined collaboration, GNO (Gallium Neutrino Observatory) resumed the observations.

3.2 Kamiokande and Super-Kamiokande

Kamiokande and Super-Kamiokande in Japan are real-time experiments utilizing νe scattering

$$\nu_x + e^- \rightarrow \nu_x + e^- \quad (5)$$

in a large water-Cherenkov detector. It should be noted that the reaction Eq. (5) is sensitive to all active neutrinos, $x = e, \mu,$ and τ . However, the sensitivity to ν_μ and ν_τ is much smaller than the sensitivity to ν_e , $\sigma(\nu_{\mu,\tau}e) \approx 0.16 \sigma(\nu_e e)$. The solar-neutrino flux measured via νe scattering is deduced assuming no neutrino oscillations.

These experiments take advantage of the directional correlation between the incoming neutrino and the recoil electron. This feature greatly helps the clear separation of the solar-neutrino signal from the background. Due to the high thresholds (7 MeV in Kamiokande and 5 MeV at present in Super-Kamiokande) the experiments observe pure ${}^8\text{B}$ solar neutrinos because *hep* neutrinos contribute negligibly according to the SSM.

The Kamiokande-II Collaboration started observing ${}^8\text{B}$ solar neutrinos at the beginning of 1987. Because of the strong directional correlation of νe scattering, this result gave the first direct evidence that the Sun emits neutrinos [22] (no directional information is available in radiochemical solar-neutrino experiments). The observed solar-neutrino flux was also significantly less than the SSM prediction. In addition, Kamiokande-II obtained the energy spectrum of recoil electrons and the fluxes separately measured in the daytime and nighttime. The Kamiokande-II experiment came to an end at the beginning of 1995.

Super-Kamiokande is a 50-kton second-generation solar-neutrino detector, which is characterized by a significantly larger counting rate than the first-generation experiments. This experiment started observation in April 1996. The solar-neutrino flux was measured as a function of zenith angle and recoil-electron energy [18]. The average solar-neutrino flux was smaller than, but consistent with, the Kamiokande-II result [17]. The observed day-night asymmetry was $A_{\text{DN}} = \frac{\text{Day} - \text{Night}}{0.5(\text{Day} + \text{Night})} = -0.021 \pm 0.020^{+0.013}_{-0.012}$. No indication of spectral distortion was observed.

In November 2001, Super-Kamiokande suffered from an accident in which substantial number of photomultiplier tubes were lost. The detector was rebuilt within a year with about half of the original number of photomultiplier tubes. The experiment with the detector before the accident is now called Super-Kamiokande-I, and that after the accident is called Super-Kamiokande-II.

3.3 SNO

In 1999, a new real time solar-neutrino experiment, SNO, in Canada started observation. This experiment uses 1000 tons of ultra-pure heavy water (D₂O) contained in a spherical acrylic vessel, surrounded by an ultra-pure H₂O shield. SNO measures ⁸B solar neutrinos via the reactions

$$\nu_e + d \rightarrow e^- + p + p \quad (6)$$

and

$$\nu_x + d \rightarrow \nu_x + p + n, \quad (7)$$

as well as νe scattering, Eq. (5). The CC reaction, Eq. (6), is sensitive only to electron neutrinos, while the NC reaction, Eq. (7), is sensitive to all active neutrinos.

The Q -value of the CC reaction is -1.4 MeV and the electron energy is strongly correlated with the neutrino energy. Thus, the CC reaction provides an accurate measure of the shape of the ⁸B solar-neutrino spectrum. The contributions from the CC reaction and νe scattering can be distinguished by using different $\cos \theta_\odot$ distributions where θ_\odot is the angle of the electron momentum with respect to the direction from the Sun to the Earth. While the νe scattering events have a strong forward peak, CC events have an approximate angular distribution of $1 - 1/3 \cos \theta_\odot$.

The threshold of the NC reaction is 2.2 MeV. In the pure D₂O, the signal of the NC reaction is neutron capture in deuterium, producing a 6.25-MeV γ -ray. In this case, the capture efficiency is low and the deposited energy is close to the detection threshold of 5 MeV. In order to enhance both the capture efficiency and the total γ -ray energy (8.6 MeV), 2 tons of NaCl were added to the heavy water in the second phase of the experiment. In addition, installation of discrete ³He neutron counters is planned for the NC measurement in the third phase.

In 2001, SNO published the initial results on the measurement of the ⁸B solar-neutrino flux via CC reaction [2]. The electron energy spectrum and the $\cos \theta_\odot$ distribution were also measured. The spectral shape of the electron energy was consistent with the expectations for an undistorted ⁸B solar-neutrino spectrum.

SNO also measured the ^8B solar-neutrino flux via νe scattering. Though the latter result had poor statistics, it was consistent with the high-statistics Super-Kamiokande result. Thus, the SNO group compared their CC result with Super-Kamiokande’s νe scattering result, and obtained evidence of an active non- ν_e component in the solar-neutrino flux, as further described in Sec. 3.5.

Later, in April, 2002, SNO reported the first result on the ^8B solar-neutrino flux measurement via NC reaction [4]. The total flux measured via NC reaction was consistent with the solar-model predictions (see Table 2). Also, the SNO’s CC and νe scattering results were updated [4]. These results were consistent with the earlier results [2].

Further, the day and night energy spectra were measured and the day-night asymmetry of the ν_e flux measured with CC events was presented [23]. Assuming an undistorted ^8B spectrum, the asymmetry was $A_{\text{DN}} = \frac{\text{Day} - \text{Night}}{0.5(\text{Day} + \text{Night})} = -0.140 \pm 0.063^{+0.015}_{-0.014}$. With an additional constraint of no asymmetry for the total flux of active neutrinos, the asymmetry was found to be $-0.070 \pm 0.049^{+0.013}_{-0.012}$.

The SNO Collaboration made a global analysis (see Sect. 3.6) of the SNO’s day and night energy spectra together with the data from other solar-neutrino experiments. The results strongly favored the LMA solution, with the LOW solution allowed at 99.5% confidence level [23]. (In most of the similar global analyses, the VAC solution was also allowed at 99.9 ~ 99.73% confidence level, see Sect. 3.6.) For the LMA solution (and also for the LOW solution), the maximal mixing was excluded at $> 3\sigma$.

Recently, in September, 2003, SNO has released the results of solar-neutrino flux measurements with dissolved NaCl in the heavy water. The results from the “salt phase” are described in Sect. 5.

3.4 Comparison of Experimental Results with Solar-Model Predictions

It is clear from Table 2 that the results from all the solar-neutrino experiments, except the SNO’s NC result, indicate

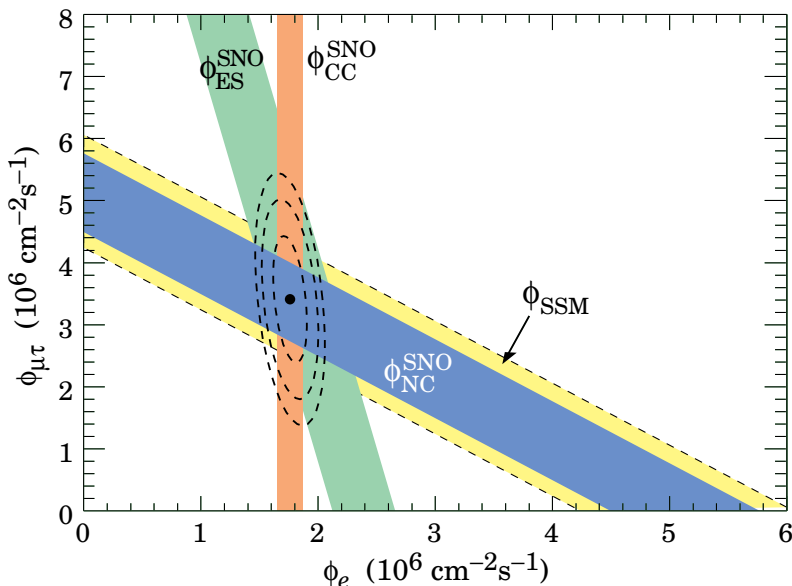


Figure 2: Fluxes of ${}^8\text{B}$ solar neutrinos, $\phi(\nu_e)$, and $\phi(\nu_\mu \text{ or } \tau)$, deduced from the SNO’s charged-current (CC), ν_e elastic scattering (ES), and neutral-current (NC) results for pure D_2O . The standard solar model prediction [9] is also shown. The bands represent the 1σ error. The contours show the 68%, 95%, and 99% joint probability for $\phi(\nu_e)$ and $\phi(\nu_\mu \text{ or } \tau)$. This figure is courtesy of K.T. Lesko (LBNL). See full-color version on color pages at end of book.

significantly less flux than expected from the BP2000 SSM [9] and the Turck-Chieze *et al.* solar model [10].

There has been a consensus that a consistent explanation of all the results of solar-neutrino observations is unlikely within the framework of astrophysics using the solar-neutrino spectra given by the standard electroweak model. Many authors made solar model-independent analyses constrained by the observed solar luminosity [24–28], where they attempted to fit the measured solar-neutrino capture rates and ${}^8\text{B}$ flux with normalization-free, undistorted energy spectra. All these attempts only obtained solutions with very low probabilities.

The data therefore suggest that the solution to the solar-neutrino problem requires nontrivial neutrino properties.

3.5 Evidence for Solar Neutrino Oscillations

Denoting the ^8B solar-neutrino flux obtained by the SNO's CC measurement as $\phi_{\text{SNO}}^{\text{CC}}(\nu_e)$ and that obtained by the Super-Kamiokande νe scattering as $\phi_{\text{SK}}^{\text{ES}}(\nu_x)$, $\phi_{\text{SNO}}^{\text{CC}}(\nu_e) = \phi_{\text{SK}}^{\text{ES}}(\nu_x)$ is expected for the standard neutrino physics. However, SNO's initial data [2] indicated

$$\phi_{\text{SK}}^{\text{ES}}(\nu_x) - \phi_{\text{SNO}}^{\text{CC}}(\nu_e) = (0.57 \pm 0.17) \times 10^6 \text{ cm}^{-2}\text{s}^{-1}. \quad (8)$$

The significance of the difference was $> 3\sigma$, implying direct evidence for the existence of a non- ν_e active neutrino flavor component in the solar-neutrino flux. A natural and most probable explanation of neutrino flavor conversion is neutrino oscillation. Note that both the SNO [2] and Super-Kamiokande [3] flux results were obtained by assuming the standard ^8B neutrino spectrum shape. This assumption was justified by the measured energy spectra in both of the experiments.

The SNO's results for pure D_2O , reported in 2002 [4], provided stronger evidence for neutrino oscillation than Eq. (8). The fluxes measured with CC, ES and NC events were

$$\phi_{\text{SNO}}^{\text{CC}}(\nu_e) = (1.76_{-0.05}^{+0.06} \pm 0.09) \times 10^6 \text{ cm}^{-2}\text{s}^{-1}, \quad (9)$$

$$\phi_{\text{SNO}}^{\text{ES}}(\nu_x) = (2.39_{-0.23}^{+0.24} \pm 0.12) \times 10^6 \text{ cm}^{-2}\text{s}^{-1}, \quad (10)$$

$$\phi_{\text{SNO}}^{\text{NC}}(\nu_x) = (5.09_{-0.43}^{+0.44+0.46}) \times 10^6 \text{ cm}^{-2}\text{s}^{-1}. \quad (11)$$

Eq. (11) is a mixing-independent result and therefore tests solar models. It shows very good agreement with the ^8B solar-neutrino flux predicted by the BP2000 SSM [9] and that predicted by Turck-Chieze *et al.* model [10]. The fluxes $\phi(\nu_e)$ and $\phi(\nu_\mu \text{ or } \tau)$ deduced from these results were remarkably consistent as can be seen in Fig. 2. The resultant flux of non- ν_e active neutrinos, $\phi(\nu_\mu \text{ or } \tau)$, was

$$\phi(\nu_\mu \text{ or } \tau) = (3.41_{-0.64}^{+0.66}) \times 10^6 \text{ cm}^{-2}\text{s}^{-1} \quad (12)$$

where the statistical and systematic errors were added in quadrature. This $\phi(\nu_\mu \text{ or } \tau)$ was 5.3σ above 0.

3.6. Pre-KamLAND Global Analyses of the Solar Neutrino Data

A global analysis of the solar-neutrino data essentially uses all the independent solar-neutrino data that are available when the analysis is made to determine the globally allowed regions in terms of two neutrino oscillations either in vacuum or in matter. A number of pre-SNO global analyses of the solar-neutrino data yielded various solutions. (For example, see Ref. [29].) With the SNO's CC and NC measurements, various global analyses [30–36] showed that LMA was the most favored solution, but either or both of the two other solutions, LOW (low probability or low mass) and VAC (vacuum), were marginally allowed at $99.9 \sim 99.73\%$ confidence level. These global analyses mostly differ in the statistical treatment of the data.

Typical parameter values [34] corresponding to these solutions are

- LMA: $\Delta m^2 = 5.5 \times 10^{-5} \text{ eV}^2$, $\tan^2 \theta = 0.42$
- LOW: $\Delta m^2 = 7.3 \times 10^{-8} \text{ eV}^2$, $\tan^2 \theta = 0.67$
- VAC: $\Delta m^2 = 6.5 \times 10^{-10} \text{ eV}^2$, $\tan^2 \theta = 1.33$.

It should be noted that all these solutions have large mixing angles. SMA (small mixing angle) solution (typical parameter values [34] are $\Delta m^2 = 5.2 \times 10^{-6} \text{ eV}^2$ and $\tan^2 \theta = 1.1 \times 10^{-3}$) was once favored, but after SNO it was excluded at $> 3\sigma$ [30–36].

4. KamLAND and Combined Oscillation Analysis

KamLAND is a 1-kton ultra-pure liquid scintillator detector located at the old Kamiokande's site in Japan. Although the ultimate goal of KamLAND is observation of ${}^7\text{Be}$ solar neutrinos with much lower energy threshold, the initial phase of the experiment is a long baseline (flux-weighted average distance of $\sim 180 \text{ km}$) neutrino oscillation experiment using $\bar{\nu}_e$'s emitted from power reactors. The reaction $\bar{\nu}_e + p \rightarrow e^+ + n$ is used to detect reactor $\bar{\nu}_e$'s and delayed coincidence with 2.2 MeV γ -ray from neutron capture on a proton is used to reduce the backgrounds.

With the reactor $\bar{\nu}_e$'s energy spectrum ($< 8 \text{ MeV}$) and an analysis threshold of 2.6 MeV, this experiment has a sensitive Δm^2 range down to $\sim 10^{-5} \text{ eV}^2$. Therefore, if the LMA

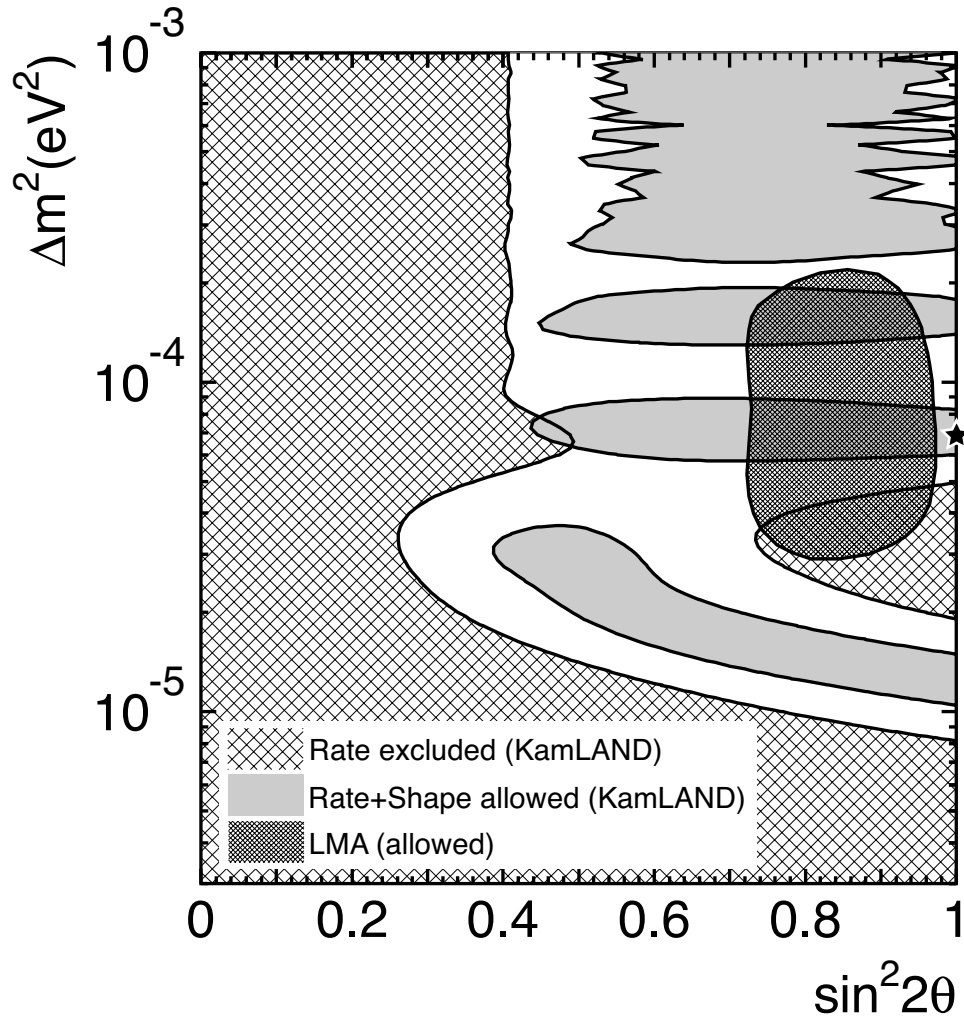


Figure 3: Excluded regions of neutrino oscillation parameters for the rate analysis and allowed regions for the combined rate and shape analysis from KamLAND at 95% confidence level. The 95% confidence-level allowed region of the LMA solution taken from a global analysis by Fogli *et al.* [34] is also shown. The star shows the best fit to the KamLAND data in the physical region: $\sin^2 2\theta = 1.0$ and $\Delta m^2 = 6.9 \times 10^{-5} \text{ eV}^2$. All regions look identical under $\theta \leftrightarrow (\pi/2 - \theta)$ except for the LMA region from solar-neutrino experiments. This figure is courtesy of K. Inoue (Tohoku University).

solution is the real solution of the solar neutrino problem, KamLAND should observe reactor $\bar{\nu}_e$ disappearance, assuming CPT invariance.

The first KamLAND results [7] with live time of 145 days were reported in December 2002. The ratio of observed to expected (assuming no neutrino oscillation) number of events was

$$\frac{N_{\text{obs}} - N_{\text{BG}}}{N_{\text{NoOsc}}} = 0.611 \pm 0.085 \pm 0.041. \quad (13)$$

with obvious notation. This result shows clear evidence of event deficit expected from neutrino oscillation. The 95% confidence level allowed regions shown in Fig. 3 are obtained from the oscillation analysis with the observed event rates and positron spectrum shape. In this figure, the allowed region for the LMA solution from a global analysis [34] of the solar-neutrino data is also shown. There are two bands of regions allowed by both solar and KamLAND data. The LOW and VAC solutions are excluded by the KamLAND results.

A combined global solar and KamLAND analysis shows that the LMA is a unique solution to the solar neutrino problem with $> 5\sigma$ confidence level [37]. The 99% confidence level allowed region from combined analyses [37–45] splits into two subregions. At $> 3\sigma$ these subregions become connected.

5. SNO Salt Phase Results

The SNO Collaboration recently reported the total ^8B solar-neutrino flux measured via NC reaction with NaCl dissolved in the detector heavy water [8]. The accuracy in the flux measurement has improved compared to the previous measurements thanks to the enhanced sensitivity to NC reactions (see Table 2). These results further constrain the allowed region of the LMA solution (see Fig. 4). A global analysis of the solar-neutrino data combined with the KamLAND data has shrunk the allowed region to the lower Δm^2 band at 99% confidence level with the best fit point at $\Delta m^2 = 7.1_{-0.6}^{+1.2} \times 10^{-5} \text{ eV}^2$ and $\theta = 32.5_{-2.3}^{+2.4}$ degrees [8]. The maximal mixing is now excluded at $> 5\sigma$ confidence level [8]. Other combined analyses give consistent results [46–51].

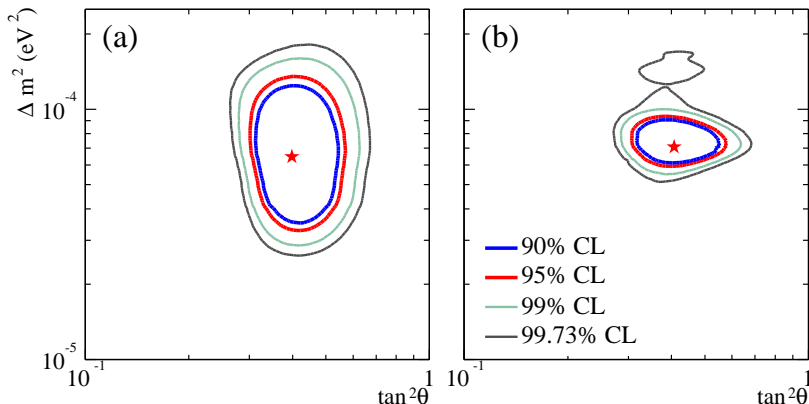


Figure 4: Global neutrino oscillation contours given by the SNO Collaboration assuming that the ${}^8\text{B}$ neutrino flux is free and the ${}_{\text{hep}}$ neutrino flux is fixed. (a) Solar global analysis. (b) Solar global + KamLAND. For details, see Ref. [8]. See full-color version on color pages at end of book.

6. Future Prospects

Now that the solar-neutrino problem has been essentially solved, what are the future prospects of the solar-neutrino experiments?

From the particle-physics point of view, precise determination of the oscillation parameters and search for non-standard physics such as a small admixture of a sterile component in the solar-neutrino flux will be still of interest. To determine Δm^2 more precisely, further KamLAND exposure to the reactor neutrinos will be most powerful [46,53]. More precise NC measurements by SNO will contribute in reducing the uncertainty of the mixing angle [51,53]. Measurements of the pp flux to an accuracy comparable to the quoted accuracy ($\pm 1\%$) of the SSM calculation will significantly improve the precision of the mixing angle [46,53].

An important task of the future solar neutrino experiments is further tests of the SSM by measuring monochromatic ${}^7\text{Be}$ neutrinos and fundamental pp neutrinos. The ${}^7\text{Be}$ neutrino flux will be measured by a new experiment, Borexino, at Gran Sasso

via νe scattering in 300 tons of ultra-pure liquid scintillator with a detection threshold as low as 250 keV. KamLAND will also observe ${}^7\text{Be}$ neutrinos if the detection threshold can be lowered to a level similar to that of Borexino.

For the detection of pp neutrinos, various ideas for the detection scheme have been presented. However, no experiments have been approved yet, and extensive R&D efforts are still needed for any of these ideas to prove its feasibility.

References

1. D. Davis, Jr., D.S. Harmer, and K.C. Hoffman, *Phys. Rev. Lett.* **20**, 1205 (1968).
2. Q.R. Ahmad *et al.*, *Phys. Rev. Lett.* **87**, 071301 (2001).
3. Y. Fukuda *et al.*, *Phys. Rev. Lett.* **86**, 5651 (2001).
4. Q.R. Ahmad *et al.*, *Phys. Rev. Lett.* **89**, 011301 (2002).
5. L. Wolfenstein, *Phys. Rev.* **D17**, 2369 (1978).
6. S.P. Mikheyev and A. Yu. Smirnov, *Sov. J. Nucl. Phys.* **42**, 913 (1985).
7. K. Eguchi *et al.*, *Phys. Rev. Lett.* **90**, 021802 (2003).
8. S.N. Ahmed *et al.*, [nucl-ex/03090034](#).
9. J.N. Bahcall, M.H. Pinsonneault, and S. Basu, *Astrophys. J.* **555**, 990 (2001).
10. S. Turck-Chieze *et al.*, *Astrophys. J.* **555**, L69 (2001).
11. A.R. Junghans *et al.*, *Phys. Rev. Lett.* **88**, 041101 (2002).
12. J.N. Bahcall, M.C. Gonzalez-Garcia, and C. Peña-Garay, *JHEP* **04**, 007 (2002).
13. B.T. Cleveland *et al.*, *Ap. J.* **496**, 505 (1998).
14. W. Hampel *et al.*, *Phys. Lett.* **B447**, 127 (1999).
15. M. Altmann *et al.*, *Phys. Lett.* **B490**, 16 (2000).
16. J.N. Abdurashitov *et al.*, *Sov. Phys. JETP* **95**, 181 (2002).
17. Y. Fukuda *et al.*, *Phys. Rev. Lett.* **77**, 1683 (1996).
18. Y. Fukuda *et al.*, *Phys. Lett.* **B539**, 179 (2002).
19. P. Anselmann *et al.*, *Phys. Lett.* **B285**, 376 (1994).
20. A.I. Abazov *et al.*, *Phys. Rev. Lett.* **67**, 3332 (1991).
21. J.N. Abdurashitov *et al.*, *Phys. Lett.* **B328**, 234 (1994).
22. K.S. Hirata *et al.*, *Phys. Rev. Lett.* **63**, 16 (1989).
23. Q.R. Ahmad *et al.*, *Phys. Rev. Lett.* **89**, 011302 (2002).
24. N. Hata, S. Bludman, and P. Langacker, *Phys. Rev.* **D49**, 3622 (1994).

25. N. Hata and P. Langacker, Phys. Rev. **D52**, 420 (1995).
26. N. Hata and P. Langacker, Phys. Rev. **D56**, 6107 (1997).
27. S. Parke, Phys. Rev. Lett. **74**, 839 (1995).
28. K.M. Heeger and R.G.H. Robertson, Phys. Rev. Lett. **77**, 3720 (1996).
29. J.N. Bahcall, P.I. Krastev, and A.Yu. Smirnov, JHEP, 05, 015 (2001).
30. V. Barger *et al.*, Phys. Lett. **B537**, 179 (2002).
31. A. Bandyopadhyay *et al.*, Phys. Lett. **B540**, 14 (2002).
32. J.N. Bahcall, C.M. Gonzalez-Garcia, and C. Peña-Garay, JHEP 07, 054 (2002).
33. A. Strumia *et al.*, Phys. Lett. **B541**, 327 (2002).
34. G.L. Fogli *et al.*, Phys. Rev. **D66**, 053010 (2002).
35. P.C. de Holanda and A. Yu Smirnov, Phys. Rev. **D66**, 113005 (2002).
36. M. Maltoni *et al.*, Phys. Rev. **D67**, 013011 (2003).
37. J.N. Bahcall, M.C. Gonzalez-Garcia, and C. Peña-Garay, JHEP 02, 009 (2003).
38. G.L. Fogli *et al.*, Phys. Rev. **D67**, 073002 (2003).
39. V. Barger and D. Marfatia Phys. Lett. **B555**, 144 (2003).
40. M. Maltoni *et al.*, Phys. Rev. **D67**, 093003 (2003).
41. A. Bandyopadhyay *et al.*, Phys. Lett. **B559**, 121 (2003).
42. P.C. de Holanda and A. Yu Smirnov, JCAP 02, 001 (2003).
43. A.B. Balantekin and H. Yüksel, J. Phys. **G29**, 665 (2003).
44. H. Nunokawa, W.J.C. Tevas, and R. Zukanovich Funchal, Phys. Lett. **B562**, 28 (2003).
45. P. Aliani *et al.*, hep-ph/0212212.
46. J.N. Bahcall and C. Peña-Garay, hep-ph/0305159.
47. A.B. Balantekin and H. Yüksel, hep-ph/0309079.
48. G.L. Fogli *et al.*, hep-ph/0309100.
49. M. Maltoni *et al.*, hep-ph/0309130.
50. P. Aliani *et al.*, hep-ph/0309156.
51. A. Bandyopadhyay *et al.*, hep-ph/0309174.
52. P.C. de Holanda and A. Yu Smirnov, hep-ph/0309299.
53. A. Bandyopadhyay, S. Choubey, and S. Goswami, Phys. Rev. **D67**, 113011 (2003).